metals

MDPI

Article

Influence of Welding on Dynamic Fracture Toughness of Strenx 700MC Steel

Eva Schmidová [1]*, Fatih Bozkurt [1], Bohumil Culek [1], Sunil Kumar MR[1], Lenka Kuchariková [2] and Milan Uhríčik [2]

[1] Faculty of Transport Engineering, Department of Mechanic and Materials, University of Pardubice, Studentská 95, 532 10 Pardubice, Czech Republic; st43852@student.upce.cz; bohumil.culek@upce.cz; sunilmr21@gmail.com

[2] Faculty of Mechanical Engineering, Department of Materials Engineering, University of Žilina, Univerzitná 8215/1, 010 26 Žilina, Slovakia; lenka.kucharikova@fstroj.uniza.sk; milan.uhricik@fstroj.uniza.sk

* Correspondence: eva.schmidova@upce.cz; Tel.: +420-466-036-444

Received: date; Accepted: date; Published: date

Abstract: The use of high-strength steels after thermo-mechanical treatment in the construction of means of transport is one way to increase passive safety capacity and useful load. One of the decisive criteria for the application of this type of steel is their stability against the internal defects, especially in connection with the welding. Currently, a major limiting factor for the wider use of high-strength steels is missing safety data according to the criteria of fracture mechanics; semi-products with a limited thickness do not allow standard tests under plane strain conditions. This paper presents a specific procedure for fracture toughness evaluation using round bar samples with a circumferential fatigue crack. A new procedure for dynamic fracture toughness testing of uniaxial load was designed and implemented. Comparative tests of Strenx 700MC steel with standard structural steel were performed, and the benefits of the new testing procedure are presented there. Fractographic and metallographic analyses describe a specific fracture behaviour controlled by internal structural heterogeneity. Limiting degradation process due to welding was identified by experimental analysis. To achieve a homogeneous zone for the requirements of fracture toughness tests, simulation of the welding influence was performed. The obtained results thus describe changes in fracture toughness at increased load speed including the critical zone of the weld joint.

Keywords: dynamic fracture toughness; high strength steels; fracture behavior; welding influence; heat-affected zone; simulation of welding; heterogeneous carbide precipitation

1. Introduction

The use of high-strength steel in the construction of means of transport has grown over the years. The driving force is both technical and environmental, where passive safety requirements have brought about the development of ultrahigh-strength steel based on specific processes of dynamic strengthening during the crash-strain rate [1, 2]. Particularly for application in means of transport, a variety of high-strength steels meet the increasing requirements for lightweight construction and therefore for an increased efficient loading capacity and lower fuel consumption [3, 4].

An inevitable part of transport means design, mainly for safety estimation, is the use of fracture mechanics methods. Determination of fracture toughness is a way to quantify the crack sensitivity of the used material and generally grows with strength of the steels. Fracture toughness in this application is required to serve as a material property that can be transferred from laboratory tests to structural applications. In terms of that requirement, the crack-tip constraint caused by thickness, i.e.

size and configuration of fracture test specimens have a significant effect on the laboratory-measured values of fracture toughness using all approaches. In general, higher constraints result in lowered crack tip yielding and promote brittle fractures, and so lower crack propagation resistance. The plane strain fracture toughness is regarded as the lower bound value.

Despite a tendency to reduce the thickness of construction components, their real toughness is driven by the overall design, including welding joints [5-7]. This means that the true dimensions and shape, together with local structural and mechanical heterogeneities have to be considered in the analysis and final structural design. In addition, the influence of strain rate and temperature on fracture toughness needs to be understood regarding the particular application of structural components.

The essential restriction, in fact decisive for the practical application of the fracture mechanics approach to operational safety assessment, is connected with limited transferability between operational and laboratory conditions. The problem remains how to generalize the results from laboratory specimens, basically with a deep cracked dominated geometry, to an application that is likely to be shallow cracked, tension-loaded, and loaded either more slowly or more rapidly than the laboratory sample. In order to obtain conservative, constraint-independent fracture toughness measurements, all fracture test standards prescribe strict specimen geometry requirements [8]. These are targeted to produce a lower bound of fracture toughness in most cases, though the degree of conservatism is not defined [9,10]. Defined specimens – crack dimension ratios, side grooves, conservative evaluation of K, J, or CTOD – all contribute to conservative results.

One of the most effective processes to increase material resilience to critical sudden fracture is to influence the natural crack propagation through microstructural heterogeneity. The presented study is focused on the mentioned process using the one of the prospective steels for lightweight constructions – Strenx 700MC. The main objective of the experimental analyses was to obtain information about the fracture behaviour of this steel at precisely defined load parameters and also at defined initial structural steel state. Various loading rates and the impact of structural degradation by welding were included in the analyses. The primary motivation was to contribute to the understanding of the ongoing material processes and the possibilities to express them through a non-standard approach to assessing fracture toughness by using circular samples.

2. Materials and Methods

2.1. Experimental Material

The steel Strenx 700MC, used in this study, belongs to the category of microalloyed high-strength steels, widely used for trailers, containers, truck frame rails, dump truck cabs, etc. The mechanical properties of Strenx 700MC meet or exceed the requirements in EN 10149-2. Strenx 700MC is a hot-rolled structural steel with a minimum yield strength of 700 MPa, made for cold forming and intended for stronger and lighter structures.

This steel type is typical of steels with a low carbon content, an increased content of manganese, a reduced sulfur content, and the addition of microalloyed elements, see Table 1. The sum of Nb, V, and Ti = max 0.22% of steel content, and together with thermo-mechanical processing these result in grain refinement and increases in strength and toughness. Because of all the influential aspects – technical, manufacturing, economic, and environmental, this steel has good prerequisites for use in rail transport to weight reduce and increase payload.

Table 1. Chemical composition (wt. %) of the used steels

		C	**Si**	**Mn**	**P**	**S**	**Al_{tot}**	**Nb**	**V**	**Ti**
Strenx	EN 10149-2 (max.)	0.12	0.21	2.1	0.020	0.010	0.015	0.09	0.20	0.15
700MC	Sample	0.047	0.028	1.75	0.009	0.0026	0.041	0.061	0.016	0.091
S355NJ	Standard (max.)	0.23	0.05	1.60	0.05	0.05	-	-	-	-
	Sample	0.15	0.18	1.32	0.017	0.0056	0.035	-	0.0016	0.001

Today's railway framex are mainly made of material with yield strength of 235–355 MPa. Because of that, steel S355NJ (chemical composition see Table 1) was used as a referential steel for the performed experimental analyses. The real mechanical properties may significantly vary depending on rolling direction. The mechanical parameters of the studied steels in a longitudinal direction, i.e. the same as a direction of samples used for all performed analyses, are in Table 2.

Table 2. Static mechanical parameters of the used steels.

Material	Yield Strength (MPa)	Tensile Strength (MPa)
S355NJ	516	550
Strenx 700MC	623	683

2.2. Methodology of Fracture Testing

One of the ways to evaluate the dynamic fracture toughness for steel plates of limited width is a measurement of fracture toughness at impact loading rates using pre-cracked Charpy-type test pieces. Testing single-edge bend specimens (SENB), fatigue pre-cracked and loaded in three-point bending is introduced in standards ISO 26843 [11] and ASTM E 1820 [12], including the recommended shape, specimen dimensions, and fatigue pre-cracking requirements. Dynamic fracture mechanics properties determined using samples with cross-sections of 10x10 mm are comparable with conventional large-scale fracture mechanics results when the corresponding validity criteria are met. Because of the small absolute size of the Charpy specimen, this is often not the case. So the values obtained are applicable to the research and development of materials and to establishing the variation of properties with loading conditions. This methodology of testing was employed to verify the testing possibility of the used steel with defined thickness. For the dynamic test, 10x5x55 mm samples were used with a chevron notch (according to EN ISO 12737), as shown in Figure 1.

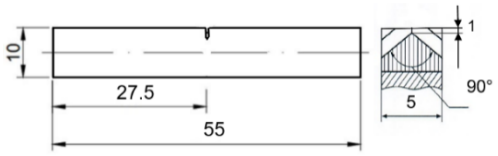

Figure 1. Chevron notched sample for dynamic fracture toughness testing.

A novel test method to study the crack resistance in mode-I loading was subsequently used. This approach enables radial pre-cracking and uniaxial static and also dynamic loading, e.g. research of strain rate sensitivity up to the standard crash rate loading [13-16]. Circumferential pre-cracked round bar test method (CCRB) is based on round specimens fatigue pre-cracked at a defined notch and loaded in a uniaxial tensile test (at different loading rates) till failure. The specimens with V-type notches with notch angles of 60° and 1 mm radial depth, mean notch radius 0.225, and dimensions displayed in Figure 2 were used in the performed analyses. The specimen was prepared from steel plates parallel to rolling.

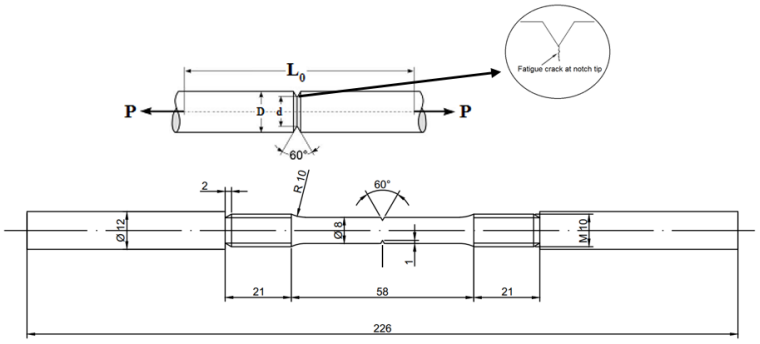

Figure 2. Round specimen for dynamic fracture toughness testing.

An R.R. Moore four-point rotating bending fatigue loading machine was used for specimen precracking as shown in Figure 3 and crack propagated radially towards the center of the specimens. The specimens were subjected to cyclic tensile–compressive loads (R_{stress} = -1). The chosen bending loading (M) had to respond to the maximum stress intensity factor K_{max} which should not exceed 60% of the minimum expected fracture toughness K_{IC} of the tested material.

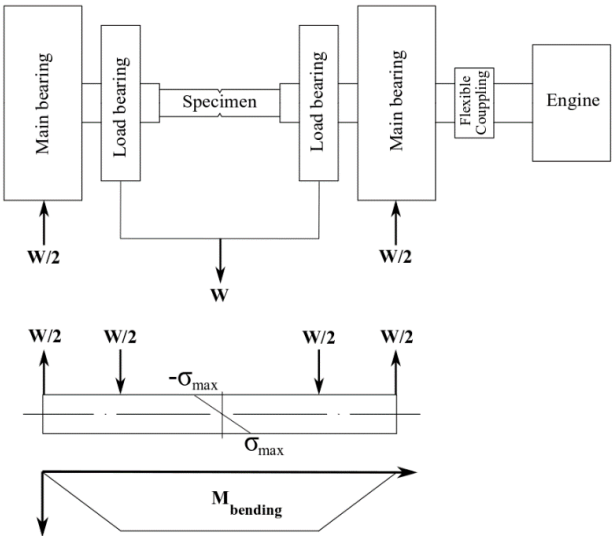

Figure 3. R. R. Moore four-point fatigue testing machine.

The pre-cracking process was controlled by a JK–1 Crack Depth Meter device, based on the measurement of the electrical resistance at the notched area. Particular resistance levels, according to the surface and initial notch geometry conditions of each samples, was measured during individual calibration processes for all samples. When a fatigue crack was detected, the specimen was ready for the static or dynamic tensile test.

For mode-I loading conditions, the pre-cracked specimen was loaded in tension at static and dynamic conditions as well. A crosshead displacement rate of 0.5 mm/min until failure was used for evaluation of static fracture response. In order to investigate the effect of the loading rate on the dynamic fracture toughness of the materials, the impact tensile tests were conducted at two different impact velocities 3.48 m/s and 5.23 m/s. In the present study, Zwick/Roell RKP 450 with PC connected with testXpert testing software was chosen to conduct the instrumented impact tensile tests. Force and crosshead displacement were recorded during the static and dynamic tensile tests as well. All tests were performed at room temperature. A minimum of three specimens of the material were tested at the same conditions for fracture toughness calculation. The maximum loads reached by each specimen were specified.

After completion of the uniaxial tests, the fracture surface of the specimen was investigated, and specified dimensions were measured with a stereo microscope as shown in Figure 4. To calculate fracture toughness, defined dimensions were machined notch depth (a_m - region A) and length of fatigue pre-crack (a_f - region B). Stabile vs. unstable fracture modes were distinguished inside the final fracture range (a_b - region C) in the case of different fracture modes action.

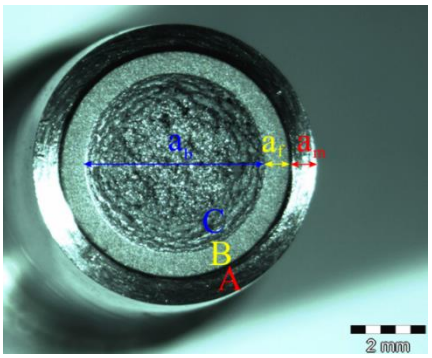

Figure 4. Defined fracture regions for fracture toughness determination.

For determination of the fracture toughness of the material, the effective diameter (d_{eff}) was stated:

$$d_{eff} = D-2(a_m + a_f) \quad (1)$$

Depending on the effective diameter (d_{eff}), unnotched section diameter (D) and maximum reached force during the impact tensile test, static fracture toughness (K_{IC}) and dynamic fracture toughness (K_{Id}) were calculated as follow

$$K_{IC}=\frac{P_f}{D^{3/2}}\left[1.72\frac{D}{d_{eff}}-1.27\right] \quad (2)$$

$$K_{Id}=\frac{P_{dmax}}{D^{3/2}}\left[1.72\frac{D}{d_{eff}}-1.27\right] \quad (3)$$

where P_f and P_{dmax} were the maximum static and dynamic fracture load, respectively. The valid range of Equation 2 and Equation 3 is $0.46<(d_{eff}/D)<0.86$.

2.3. Experimental Welding and Simulation of Impact of Welding on Samples for Fracture Tests

The above-mentioned novel approach, using round-bar specimens, was also used to provide a more detailed description and understanding of the degradation caused by welding. Welding effect evaluation was performed with the support of experimental welding and following simulation of the maximal degradation effect in area of fracture propagation.

The steel plates with dimensions of 120x300x10 mm and V-type grooves were prepared for the resistance welding process, as shown in Figure 5. Kempact 253R welding equipment was used for MAG welding (CO_2 and Ar shielding gases), with three welding passes using Böhler UNION NiMoCr Ø1 mm filler wire (Table 3). Heat input for each welding pass was between 1.1 and 1.5 KJ/mm, no heat treatment process such as stress relief annealing was carried out after or before the welding process.

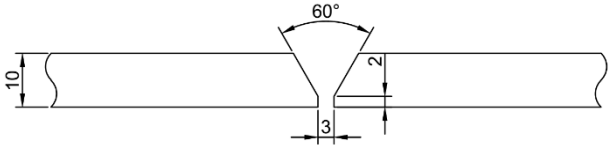

Figure 5. Details of V type configuration and dimensions of Strenx 700MC plate.

Table 3. Chemical composition (wt. %) of filler wire Böhler UNION NiMoCr Ø1.

C	Si	Mn	Cr	Mo	Ni
0.08	0.60	1.70	0.20	0.50	1.50

Simulation of welding heat effect at Strenx 700MC steel was carried out for two reasons. The first reason was the potential presence of microscopic defects that cannot be totally excluded and that affect the results of any weld joint tests. The purpose of the analyses was not to verify the technology itself, but to examine the degradation effect on the material in question, its substance and its influence on dynamic fracture behaviour.

Secondly, the welding effect simulation allows the creation of a geometrically optimised heat-affected zone (HAZ) for fracture toughness analysis. As an accurate orientation of the developing crack to the zone with the maximum degradation impact of the welding is necessary for these tests, this area must be structurally homogeneous throughout the tested cross section. The simulation allows the controlled preparation of much wider critical HAZ sublayers with typical heat levels and corresponding microstructural effects.

The real weld joint evaluation was used to identify the HAZ sublayer critical to the initial strength of the steel. Hardness measurement and microstructural evaluation served as parameters for identifying the critical degradation effects of the used experimental welding technology as well as for the validation of the used simulation process. The minimum hardness value of the real welding specimen showed a critical temperature, and the parameters of the welding simulation were specified. A welding simulation was performed using WTU 315-3 welding equipment. The specimens made for fracture analyses were heated by an electric arc over copper rings. During the welding simulation process, the temperature change over time was recorded by a Omega HH309A four-channel data logger thermometer. The specimen before and after the welding simulation process is shown in Figure 6.

Figure 6. Heating the notched area of the round bar samples.

3. Results

3.1. Verification Analysis of Welding Simulation

As a first step, complex material analyses of experimentally welded Strenx 700MC steel were performed to identify the critical sublayer of HAZ in terms of structural degradation and to describe the involved degradation process. The local differences in hardness have shown the weakest area of welding joint and the most intensive degradation effect of welding at the used type of high-strength steel. Identification of the most softened sublayer provided information about the critical temperature level for the design of the weld thermal influence simulation.

The Vickers hardness measurement of the welded specimen (according to EN ISO 6507-1) was conducted perpendicularly to the weld joint axis, on the HV1 scale, with 0.2 mm interval – see Figure 7. The hardness measurement indicated the lowest values in the sublayer of the outer part of the grain refinement zone (236 HV1).

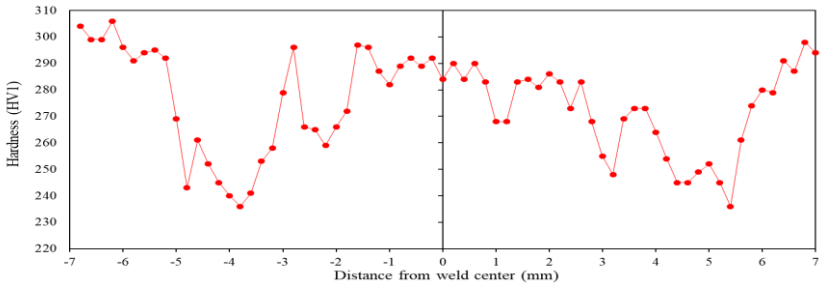

Figure 7. HV1 hardness vs. distance from weld center for welded Strenx 700MC specimen.

A simulation of the degradation process was designed based on analyses of experimental welding process influences. During the thermal cycle simulation, the specimen, with geometry for static or dynamic uniaxial tests, was heated to a maximum temperature of 800 °C and held at this temperature for 5 seconds; the temperature was recorded as a function of time. For validation of the used simulation, the thermal cycle influence was evaluated by metallography analyses and hardness measurement. The samples were extracted from the longitudinal axis of the circumferentially round bar specimen of the Strenx 700MC steel and prepared by a standard metallographic preparation process. Stable hardness values at the notch tip presented very important results in terms of material homogeneity in the fracture plane, i.e. they prove the suitable conditions for the fracture resistance evaluation. The hardness values varied from 216 HV1 to 233 HV1 and the mean value was approximately 225 HV1. As mentioned above, the main aim was to approach the lowest hardness level (236 HV1), which was induced in the experimental welding sample of Strenx 700MC. In this way, the suitability of the simulation used to assess the degradation process due to welding was verified.

3.2. Metallography Evaluation of Related Structural Effects

The microstructure of uninfluenced Strenx700MC steel consists of a fine-grained polygonal ferrite with a limited amount of pearlite. Outstanding strength and impact toughness are a result of the fine-grained microstructure in combination with thermo-mechanical rolling in a hot strip mill. Typical microstructural effects of the applied welding technology are documented in Figure 8. The ferritic structure of the test steel has shown a partial acicular morphology along with the distribution of very fine carbides (Figure 8a), which contributes to increased strength. Reaustenitisation caused a typical grain coarsening in the so-called superheated welding area adjacent to the fusion zone (Figure 8b). Grain refinement was observed in a substantial part of the HAZ (Figure 9a); in addition to the influence on the grain size, the heat input led to carbide re-precipitation. Significant distribution of relatively coarsened carbides (up to 1 μm thick) was found in the band immediately above the austenitisation temperature. On the other hand, much finer and less globularised carbides were formed in the grain-coarsened zone.

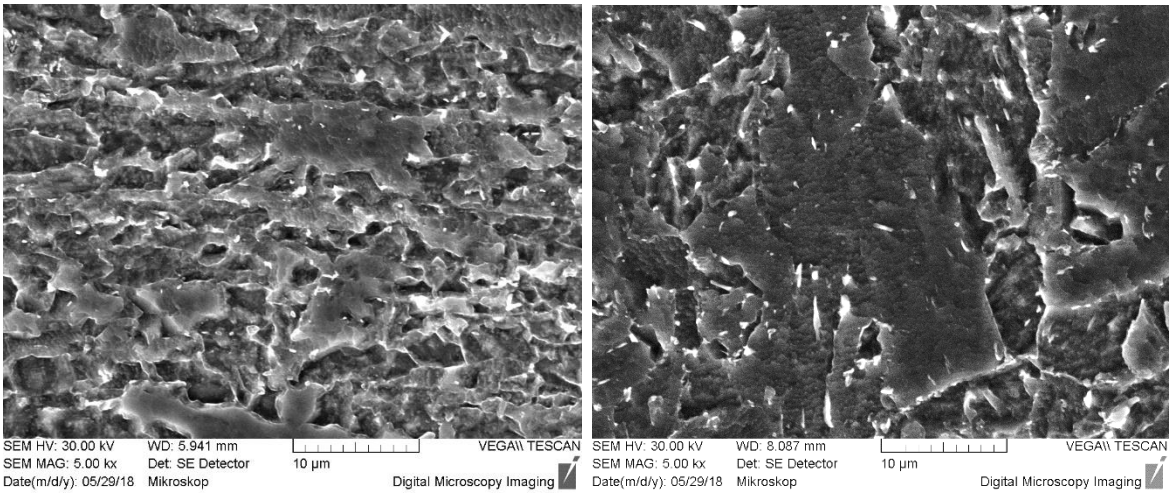

(a) (b)

Figure 8. Strenx 700MC structural changes after used welding technology influence: (a) Uninfluenced steel; (b) Fusion zone

After completion of the welding influence simulation, a sample for metallographic examination was prepared from the circumferential notched round bar specimen. Comparative structural analyses were conducted directly in the area of the notch tip, i.e. in the area of crack propagation at fracture toughness examination.

The carbide reprecipitation process was found to be the most effective degradation process by the metallography evaluation of the real welding influence. Due to that, the comparison of dissolution and re-precipitation of carbides was also an important validation effect of the performed simulation process. As shown in Figure 9b, a coarsening of the primary carbides was induced by the simulation process. This observation confirms accordance with the critical structural influence of real welding processes. The initiation of microcracks along the coarsened carbides during mechanical testing was also visible.

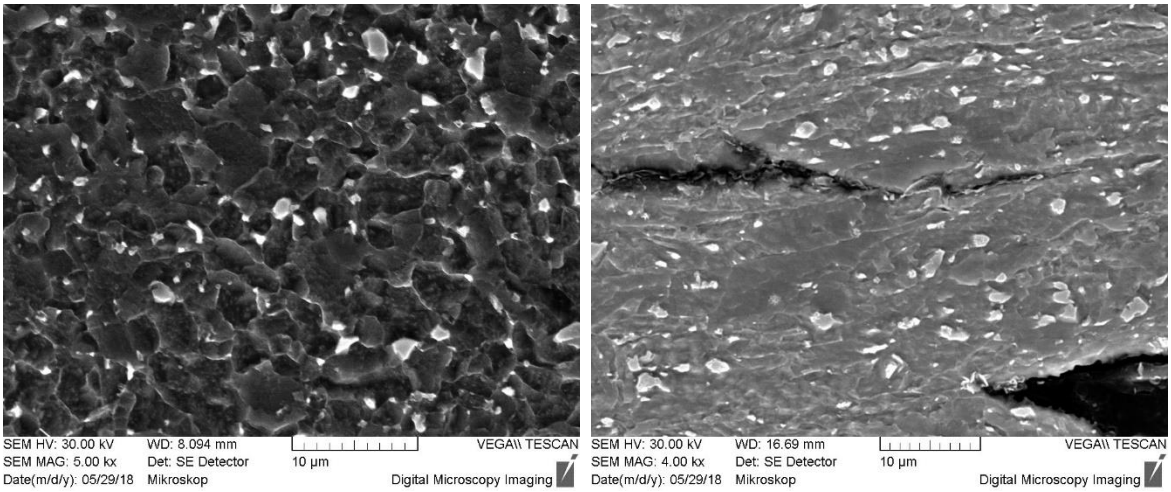

Figure 9. Carbide precipitation in the critical HAZ layer: (a) After real welding (b) After weld simulation.

3.3. Fracture Response Evaluation

Chevron-notched sample testing led to unacceptable fracture responses in all tested positions. The plane of the fracture deflected immediately as the tip of crack reached the carbide row, so the real distribution of carbides has de facto driven the following fracture plane and so influenced all the measured results, namely maximal force and total energy consumption. Figure 10a presents the influence of the position of crack deflection on the fracture resistance of Strenx 700MC steel. Furthermore, the tendency to ductile fracture evident from the detail in Figure 10b, i.e. plane deformation condition was not achieved.

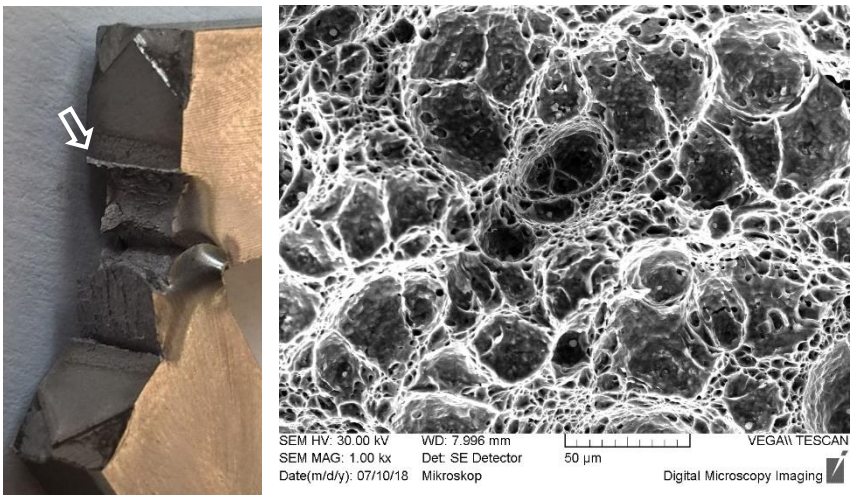

Figure 10. Fractured chevron notched samples: (a) Crack deflection due to carbide precipitation; (b) Ductile fracture mode

The results of static versus dynamic fracture toughness of the parent material, determined using the CCRB method, are listed in Table 4 compared to S355NJ steel. Dynamic values obtained at the maximal loading rate is significantly higher than compared to the static values, so a strengthening process has been involved. It points on the presence of an effective plastic zone on the tip of the moving fracture, which enables the dislocation hardening process. An increased scattering of dynamic strength and fracture toughness values was obtained at the maximal loading rate.

Table 4. Fracture response results of the Strenx 700MC at different loading rate – parent material

	Sample No	F_{max} (N)	D (mm)	a_m (mm)	a_f (mm)	d_{eff} (mm)	d_{eff}/D	K_I (MPa.m$^{1/2}$)
Static 0.02 m/s	S1	28744	7.7	0.7	0.64	5.02	0.65	58.2
	S2	31953	7.65	0.695	0.47	5.32	0.70	57.5
	S3	32243	7.61	0.69	0.38	5.47	0.72	54.5
	Average value							57
	Average value – S355NJ							45
Dynamic 3.48 m/s	D-01	43676	7.62	0.69	0.2	5.84	0.77	64
	D-02	41164	8.11	0.75	0.42	5.77	0.71	64.7
	D-03	44534	8.11	0.73	0.25	6.15	0.76	60.9
	Average value							63
	Average value – S355NJ							67
Dynamic 5.23 m/s	D-1	41484	7.59	0.695	0.3216	5.56	0.73	67.7
	D-2	40534	7.78	0.66	0.38	57	0.73	63.7
	D-3	43833	6.95	0.535	0.211	5.46	0.79	69.6
	D-4	38764	7.84	0.725	0.4865	5.42	0.69	68.1
	D-5	43510	7.8	0.72	0.49	5.38	0.69	77.3
	Average value							69
	Average value – S355NJ							69

An uneven circumference fatigue crack caused by a stripe of carbide precipitation was typical for all loading conditions. Lamellar final fracture morphology (Figure 11) was observed and evaluated in both the macro- and micro-scale to assess an increased loading rate influence on fracture behaviour.

The fracture mode in the initial phase of destruction, i.e. at interphase of the fatigue fracture, was decisive for the further propagation of fractures and so for the total energy consumption. The area of a ductile fracture mode, corresponding to the stabile crack propagation, reached a decreasing area with increasing loading rate. The transition to a final unstable fracture was more affected by the carbide phase precipitation.

The heat input of simulated welding caused significant change of static and also dynamic fracture responses; the fracture toughness values are listed in Table 5.

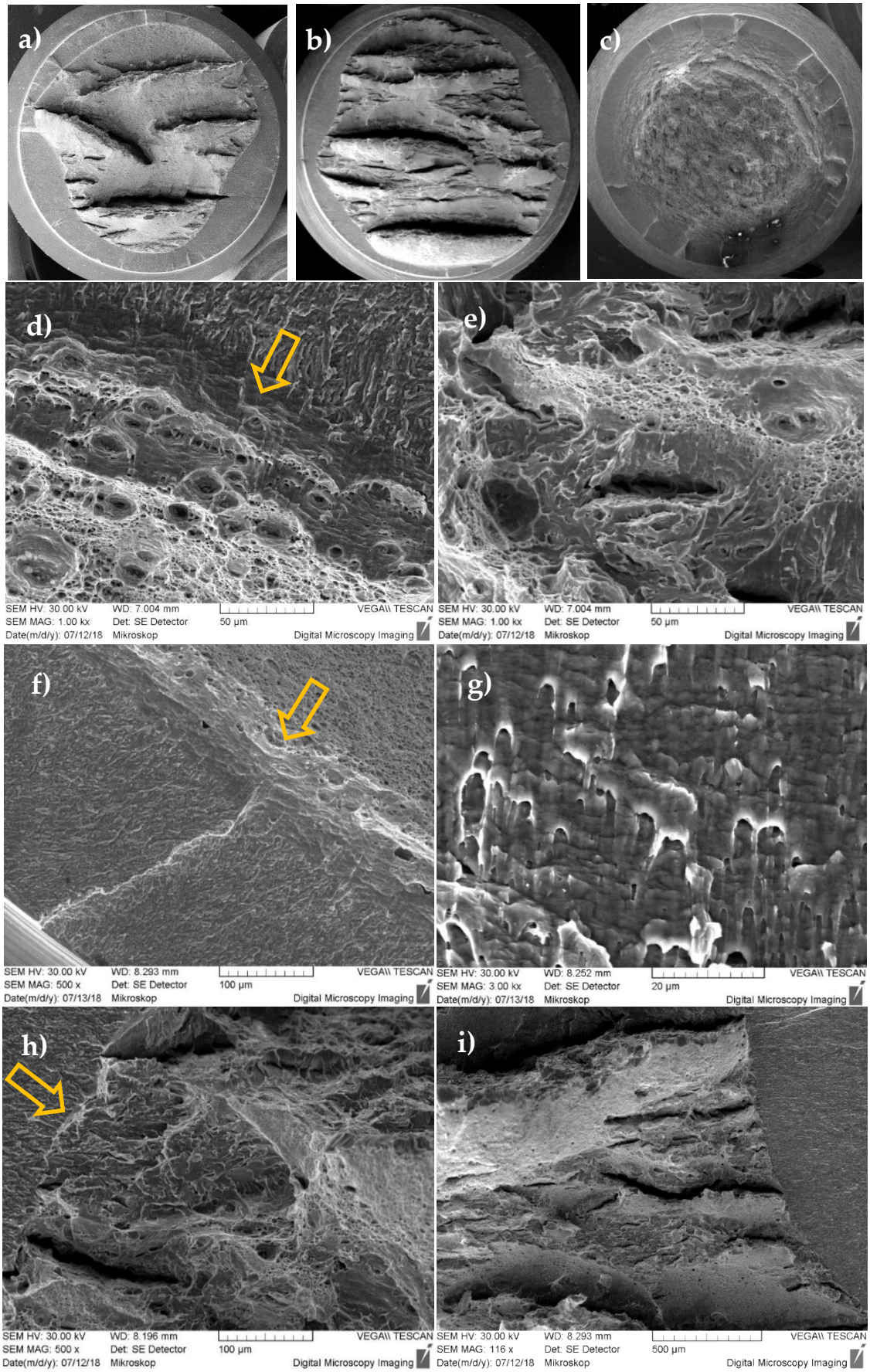

Figure 11. Fracture morphology of tested samples, a) static – uninfluenced steel, b) dynamic – uninfluenced steel, c) dynamic – HAZ, d) – e) static loaded uninfluenced steel, f) – g) uninfluenced steel loaded by impact velocity 3.48 m/s, h) – i) uninfluenced steel loaded by impact velocity 5.23 m/s.

Table 5. Strenx fracture response at different loading rate – simulated HAZ.

	Sample No	F_{max} (N)	D (mm)	a_m (mm)	a_f (mm)	d_{eff} (mm)	K_I (MPa.m$^{1/2}$)	d_{eff}/D	UTS (MPa)
Static 0.02 m/s	WS-01	34183	7.67	0.735	0.21	5.78	51.5	0.75	1303
	WS-02	24784	6.98	0.74	0.35	4.8	52.3	0.69	1370
	WS-03	24972	7.26	0.73	0.43	4.94	50.8	0.68	1303
	Average value						51.5	0.70	1325
Dynamic 5.23 m/s	DWS-01	36057	7.22	0.83	0.45	4.66	82	0.65	2114
	DWS-02	22769	7.74	0.805	1.68	2.77	118.2	0.36	3778
	DWS-03	32839	7.2	0.575	0.67	4.71	73.1	0.65	1885
	Average value						91.1	0.55	2592

4. Discussion

4.1 Structural influence by welding

The tested high-strength steel – Strenx 700MC – presents a prospective category for high-strength steel to be used in lightweight construction. The critical design aspects are related to influence of welding, so an inevitable application precondition is a deep understanding and precise evaluation all of included processes.

The potential weldability problems of high-strength steels are hydrogen cracking, lamellar tearing, loss of primary strength in the heat-affected zones, and a reduction in toughness. Hydrogen cracking does not occur for this steel because of low carbon equivalent. Performed analyses confirmed strength decreases in a narrow zone of the HAZ due to a loss of precipitation hardening. The width of the softened zone depends mainly on heat input and cooling rate. It is therefore important to limit heat input when welding these steel grades [17]. The tensile strength of Strenx 700MC, measured under the influence of different heat inputs of MAG welded joint and using different filler materials, showed a drop from about 810MPa to a minimal value of 750MPa [18].

The evaluation of the welding degradation impact was based on hardness and a structural analysis of experimental welding. The primary Strenx 700MC steel conditions were strongly influenced by the metal active gas welding method used. The hardness measurement indicated the lowest value in the sublayer at the rim of the grain refinement zone towards a lowered temperature (236 HV1). This result seemed to contradict the generally known grain refining effect. Based on detailed microstructure evaluation, it could be concluded that it was a result of a partial austenitisation process, together with the loss of both primary strengthening processes – dislocation hardening and precipitation hardening. The latter process was more effective, hence the reprecipitation of carbides leading to a substantial decrease in hardness. The minimal hardness level was an important parameter for the performed temperature cycle simulation (for the chosen maximal temperature). The region of grain coarsening was very narrow.

Microadditives of titanium, aluminium, and vanadium in this type of microalloyed steel strongly influenced the grain growth, recrystallisation of austenite, and phase transformation as well as morphology of the transformed products. The most common effect of grain coarsening – i.e. the decreasing of hardness – was overcome by partial transformation to acicular ferrite and bainite. The presence of nitrogen carbides, revealed in the HAZ by chemical microanalysis, indicated that in the investigated steel there is sufficient titanium needed to bind to free nitrogen, which is related to reduced aging processes.

The welding pool reached an almost stable hardness value. As a result, the analysis of the measurement of hardness test showed that Strenx 700MC was strongly influenced by the applied welding technology. By choosing the optimum welding parameters and method, this influence can be partially reduced but not completely eliminated [19].

4.2 Fracture behaviour under welding influence, specific conditions for methodology of fracture toughness evaluation

The static and also dynamic fracture response in the HAZ varies corresponding to the microstructural change, so it generally should be at least as good as the toughness demands in the base metal. The worst impact properties are normally obtained in the coarse-grained zone near the fusion line [20, 21].

A high amount of acicular ferrite in the analysed welding assures a combination of high strength and good impact toughness, i.e. also good dynamic fracture toughness. Welding trials (for example with electrodes OK 13.13, OK 13.29 and Spoolcord TD-T90) showed that even the most severe base metal requirements (34 J/cm2 at −40°C) can be fulfilled in the weld metal. Low heat input has to be used to get high toughness in the HAZ. For Domex 600 MC and with the most severe toughness requirement the cooling time t8/5 must be maximised to approximately 15 seconds [20, 21]. This means that that the same toughness requirement as in the base metal can be fulfilled also in the weldment for the Strenx steels if a filler metal with high toughness is used in combination with low welding heat input.

The evaluation of fracture toughness of Strenx 700MC steel is difficult due to limited plate widths. Strenx 700MC steel reaches the required mechanical parameters by thermomechanical processing, so the steel plates are limited to a width of 10 mm. The influence of welding thermal cycles on properties of HAZ of 10-mm Strenx 700MC steel plates was tested on a laboratory stand equipped with a thermovision camera and resistant heat source by Górka et al [22]. Single thermal cycles were simulated at temperatures ranging from 400 to 1300 °C (with steps of 100 °C); samples were tested using Charpy V-notched tests at −30 °C. Heating at 800 and 900 °C caused a transition to ductile fracture (from primary mixed mode fracture up to 700 °C), and at over 1000 °C brittle fracture mode was obtained.

That points out that the primary strength drop and so the significant carbide reprecipitation occur at the same critical temperature level as was considered in the presented research of dynamic fracture toughness under the influence of welding.

The high fracture toughness values together with the limited plate thicknesses (maximum 10 mm) generally imply a suppressed risk of brittle fracture. The lower three-axial stress level for the thin sheets means an increased tendency to high-energy fracture response compared to thicker plates.

A determination of fracture toughness, applicable for round-bar or square-shaped samples with reduced dimensions can be performed using chevron-notch specimens [23]. This method, according to the standard ASTM E 1304, enables the fracture toughness measurement at plane-strain conditions, where the crack is initiated directly at a chevron-shaped notch (i.e. without fatigue pre-cracking). The crack slowly advances in a chevron-shaped ligament until a critical point is reached. So the first stage of crack propagation is stable due to the decreasing of the calibration function; Y-value drops to the minimum value 'Y_{min}', at which point the maximum force is reached. The crack then becomes unstable and propagates at higher speed to the next arrest point (except in the case of fully brittle materials).

All methods based on chevron-shaped notch use covers the determination of the plane-strain fracture toughness K_I relative to the crack at the point of instability, established using maximal reached force:

$$K_I = \frac{Y_{min} F_{max}}{B\sqrt{W}} \quad (4)$$

where Y_{min} ... calibration (shape) function
F_{max} … maximal force at dynamic loading
B … sample width, W … sample high

The crack depth measure net is not included in these methods. The start of the crack extension from a fatigue pre-crack at a chevron-shaped notch is required, e.g. by ASTM E 399 [24].

The standardised pre-cracked Charpy-type test according ISO 26843-2015 was used in the first step of testing. As was mentioned above, Strenx 700MC plates are restricted to 10 mm in thickness due to thermomechanical treatment. That enables the standard Charpy samples to be prepared and – in particular – approximates the deformation conditions to the tests performed in the second step by circular specimens. In addition to that, the loading conditions in the sense of loading rate are identical with the novel method using round bar samples – up to 5.23 m/s.

The Charpy-type test with chevron-notched samples has shown the dominant presence of ductile fractures. The distinctive row of carbide precipitation in Strenx 700MC steel led to crack deflection and so de facto caused the evaluation of the tests to be impossible. So the first step of experimental analyses underlined the need for non-standard tests.

Uniaxial tests using round bar pre-cracked samples allowed the comparative static and dynamic fracture behaviour evaluation. Two main points – the effect of carbide reprecipitation and the sensitivity of steel to the strain rate – were found to be crucial parameters for prospective application. Fracture toughness values, determined at dynamic loading of up to 5.23 m/s, differ from values measured at quasi-static loading rates. Principally, it applies (and it is reported, e.g. in ISO 26843 [12]), that an increase in loading rate causes a decrease in fracture toughness when tests are performed in brittle or ductile-to-brittle fracture regimes; an increase in fracture toughness is observed in the fully ductile regime.

This generally acknowledged relation has been confirmed, ratio of strengthening of parent Strenx 700MC steel and simulated critical sublayer of HAZ at different loading rates is displayed in Figure 12. A substantial increase in sensitivity to the rate of loading was observed in HAZ. This can be explained by the re-precipitation of carbides; microstructure homogenisation led to a more intensive dislocation hardening effect.

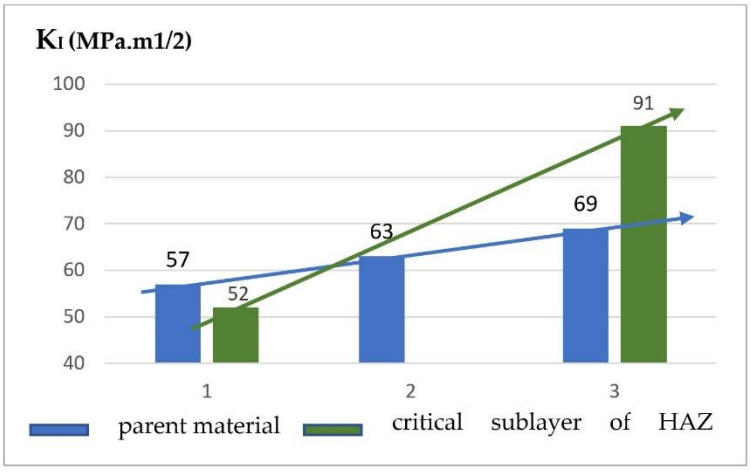

Figure 12. Fracture toughness of Strenx 700MC at strain of loading (1-0.02m/s, 2-3.48 m/s, 3-5.28 m/s)

4.3 Effect of structural heterogenity

This better understanding of steel crack sensitivity means considering crack propagation at the real microstructural level, e.g. the typical lamellar microstructure of cold-rolled high-strength steels. This is partially in contradiction to standard approaches, where for example the side grooves are used to straighten the crack propagation.

Fracture mode of steel is driven by local stress-strain conditions. The extension of the plastic zone at the tip of a crack strictly depends on many variables, such as the yield stress of the material, the crack length, the strain rate, and the thickness of the cracked component. Elastic anisotropy can be ignored, provided that the crack growth follows the original crack plane [25, 26]. Also considering the local heterogeneity in the vicinity of weld, the plane crack propagation is a precondition according to common standards [27]. In the case of significant toughness anisotropy, crack growth tends to be in the direction of a weaker zone and may not be in the direction of the initial crack even

for mode-I loading [28]. This presents, for example, a restriction for composites testing, where crack propagation appears parallel to the fibres and increases the toughness.

Also the material sensitivity to crack propagation, i.e. the fracture mechanics parameters of Strenx 700MC, are strongly driven by the orientation of the internal heterogeneity. The plate-like distribution of carbides, together with the connected depletion of carbon in the adjacent microvolumes of matrix is an influential source of the deflection of crack tip propagation. The observed fracture response revealed significant influence on primary structural heterogeneity of Strenx 700MC steel. Lamellar-like tearing was observed in the uninfluenced area; hence the obtained values of energy was over-valuated due to the branching crack propagation. Complex fracture patterns appeared in all tested samples.

The simulation of the welding degradation effect caused substantial changes in fracture response. A slight decrease in fracture toughness at static loading was observed together with more intensive dynamic strengthening. This can be explained by induced contradictional structural effects in the HAZ – carbide re-precipitation as a crucial process towards strength impairment versus microstructural homogenisation (by suppressing the row of carbide distribution) leading to increased susceptibility to deformation hardening. The performed experimental analysis of static and impact crack behaviour of simulated welded joints showed the real level of degradation caused by welding. The homogenisation effect in the HAZ is capable of suppressing the primary strip-like carbide precipitation.

The fracture behaviour of Strenx 700MC steel in the particular fracture stages is reflected in the force-displacement diagrams. Representative records at different loading rates of uninfluenced steel are displayed in Figure 13. A substantially different displacement of the final fracture presents the above-discussed effect of crack deflection due to lamellar carbide precipitation. The generally acknowledged approach to fracture toughness evaluation using round notched samples does not reflect the significant energy consumption differences in case of similar maximal force to fracture. In this specific case, however, there is no continuous development of macroplastic deformation. The decisive factor is that, as opposed to the fracture toughness test using the Charpy-type samples, the evaluation regime used here leads to a magistrate crack in the final plane and thus de facto allows for evaluation.

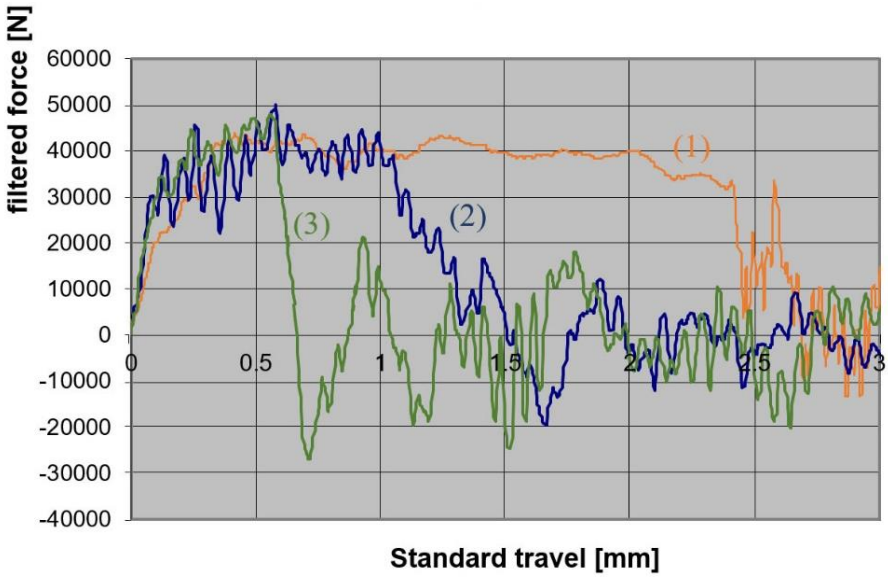

Figure 13. Typical fracture response at different loading rate (1-0.02m/s, 2-3.48 m/s, 3-5.28 m/s)

A certain case of the energy approach is a crack sensitivity assessment that has been proposed as a comparative parameter in some experimental evaluations of welding [29]. Crack sensitivity was defined as the ratio of impact energy of a Charpy V-notch specimen and the energy obtained by

pre-cracking the V-notch specimen. It is only a comparative parameter, and is influenced by crack length. Testing this principle with circular specimens provides a parameter that can be directly applied for safety assessments.

5. Conclusions

The comparative experimental analyses revealed the specifics of fracture behaviour in Strenx 700MC steel. The plane strain fracture toughness, determined by CCRB samples at static loading conditions, proved the higher values for Strenx 700MC steel as compared to S355NJ steel. The opposite ratio was observed with increasing the loading rate. The surprisingly lower dynamic fracture toughness of Strenx 700MC steel compared to the S355NJ steel was observed despite the superiority of a brittle fracture mode in S355NJ steel.

Increased fracture toughness due to increasing loading rate for both tested steels confirmed the decisive role of a plastic zone on the top of propagated crack. Intensive dynamic strengthening took place in Strenx 700MC steel in the case of primary microstructure conditions as well as after simulated degradation due to welding. The final dynamic fracture resistance of the temper-influenced zone even overcame the fracture resistance of the parent steel.

The critical sublayer of HAZ was defined as a maximal softening zone; the induced phase transformation and change of the structural components' morphology were evaluated in direct connection with fracture response in this zone. Contrary to the common limited effect of the grain-coarsening zone adjacent to the fusion line, intensive re-precipitation was induced in the partial austenitisation zone.

The methodology used to test fracture toughness provides new capabilities for fracture evaluation, and so the following advantages can be considered:

- a uniaxial loading system is the optimal mode for monitoring all the circumstances of crack development;
- the ability to apply different loading rates, e.g. using the standard Charpy hammer system up to 5.23 m/s;
- suppression of the plane stress state, typically influencing crack propagation near the surface of simple notched Charpy-type samples;
- support for the plane orientation of fracture due to the circumferential initiation of fatigue cracks.

The methodology used in this testing is effective especially for materials with heterogeneous microstructures and so with heterogeneous local mechanical parameters. Circumferential fatigue pre-cracking suppresses the fracture deflection towards to weaker microvolumes and so supports planar crack propagation. Also, the plane strain conditions are difficult to reach for Charpy-type samples. CCRB supports the plane strain condition, a transition of fracture to the main shear stress plane is suppressed significantly compared to Charpy. For a general comparison with standard methodologies used to measure fracture toughness, the conservative conditions in the sense of a limited ratio of effective diameter to outer diameter needs to be defined.

The strain rate that would correctly define the conditions for the plasticity development at the given test conditions cannot simply be determined by the deformed length. For pre-cracked specimens, it is defined by the size of the plastic zone at the front of the crack, which is de facto the material parameter of the tested steel.

Author Contributions: Conceptualization, E.S. and B.C.; methodology, E.S., F.B. and B.C.; investigation, E.S., F.B., S.K., M.U. and L.K.; resources, E.S., and F.B.; data curation, E.S., F.B. and S.K.; writing—original draft preparation, E.S. and F.B.; writing— review and editing, E.S. and F.B.; visualization, E.S. and F.B.

Funding: This research was funded by Railway Vehicle Competence Centre, project No.TE01020038.

Conflicts of Interest: The authors declare no conflict of interest

References

1. Ulewicz R, Mazur M, Bokůvka O. Structure and mechanical properties of fine-grained steels. *Periodica Polytechnica Transportation Engineerin*g **2013**, 41(2), pp.111-5.
2. Mazur, M. Fatigue properties of fine-grained steels applied in components of semitrailers. *Czasopismo Techniczne* **2016,** 4-M, pp.9-14.
3. Sperle, J., Hallberg L., Larsson J., and Groth H. The Environmental Value of High Strength Steel Structures, Environmental Research Programme for the Swedish Steel Industry, The Steel Eco-Cycle. *Scientific Report*. **2008**, Phase 1, pp. 151–171.
4. Ulewicz, R. and Szataniak, P. Fatigue Cracks of Strenx Steel. *Materials Today: Proceedings* **2016**, *3*(4), pp.1195-1198.
5. Laitila, J., Larkiola, J. and Porter, D. Effect of forced cooling on the tensile properties and impact toughness of the coarse-grained heat-affected zone of a high-strength structural steel. *Welding in the World* **2018**, *62*(1), pp.79-85.
6. Kim, S., Kang, D., Kim, T.W., Lee, J. and Lee, C. Fatigue crack growth behavior of the simulated HAZ of 800 MPa grade high-performance steel. *Materials Science and Engineering: A* **2011**, *528*(6), pp.2331-2338.
7. Antolovich, S.D., Saxena, A. and Gerberich, W.W. Fracture mechanics–An interpretive technical history. *Mechanics Research Communications* **2018**, *91*, pp.46-86.
8. ISO 26843:2015(E), Metallic Materials - Measurement of Fracture Toughness at Impact Loading Rates Using Precracked Charpy-Type Test Pieces, p. 35.
9. Leskov, V. Multi-Functional Kıc-Test Specimen for the Assessment of Different Tool- and High-Speed-Steel Properties, *Mater. Technol*. **2013**, 47(3), pp. 273–283.
10. Smith, R.J., Horn, A.J. and Sherry, A.H. Relating Charpy energy to fracture toughness in the lower transition region using a Weibull stress dependent energy scaling model. *International Journal of Pressure Vessels and Piping* **2018**, Vol. 166, pp. 72-83, ISSN 0308-0161, DOI 10.1016
11. ISO 26843:2015(E), Metallic Materials - Measurement of Fracture Toughness at Impact Loading Rates Using Precracked Charpy-Type Test Pieces.
12. ASTM Designation E1820 − 17a, 2018, "Standard Test Method for Measurement of Fracture Toughness,"
13. Londe N. V., Jayaraju T., and Rao P. R. S. Determination of Plane-Strain Fracture Toughness of AL 2014-T6 Alloy Using Circumferentially Cracked Round Bar Specimen, *Eng. E-Trans*. **2006**, (1), pp. 26–31.
14. Wilson, C.D. and Landes, J.D., Fracture toughness testing with notched round bars. *Fatigue and Fracture Mechanics:* 30th Volume. ASTM International. **2000**, 30th Volume, West Conshohocken, PA 19428-2959, pp. 69–82.
15. Londe N. V., Jayaraju, T., Naik, P., Kumar, D. and Rajashekar, C.R. Determination of fracture toughness and fatigue crack growth rate using circumferentially cracked round bar specimens of Al2014T651. *Aerospace Science and Technology* **2015**, *47*, pp.92-97.
16. Li, D.M. and Bakker, A. Fracture toughness evaluation using circumferentially-cracked cylindrical bar specimens. *Engineering fracture mechanics* **1997**, *57*(1), pp.1-11.
17. Górka, J. and Stano, S. Microstructure and Properties of Hybrid Laser Arc Welded Joints (Laser Beam-MAG) in Thermo-Mechanical Control Processed S700MC Steel. *Metals* **2018**, *8*(2), p.132.
18. Kumar, S., Nath, S.K. and Kumar, V. Continuous cooling transformation behavior in the weld coarse grained heat affected zone and mechanical properties of Nb-microalloyed and HY85 steels. *Materials & Design* **2016**, *90*, pp.177-184.
19. Shi, Y. and Han, Z. Effect of weld thermal cycle on microstructure and fracture toughness of simulated heat-affected zone for a 800 MPa grade high strength low alloy steel. *Journal of materials processing technology* **2008**, *207*(1-3), pp.30-39.
20. Eckerlid1 J., Åsell1 M., Ohlsson1 A. Use of Vanadium High-Strength Low-Alloy Steels in Trailers, In *A case study.* The steel company Tunnplåt AB **2009,** Sweden
21. Mohyla P., Hlavatý I., Tomčík P. Cause of Secondary Hardening in Cr-Mo-V Weld during Long-Term Heat Exposure. *Avtomaticheskaya Svarka* **2011**, No. 2 (694), pp. 27-30.
22. Górka J. Influence of the maximum temperature of the thermal cycle on the properties and structure of the HAZ of steel S700MC. IOSR *J. of Eng*. **2013**, 3(11), pp.22-8.
23. Grant TJ, Weber L, Mortensen A. Plasticity in Chevron-notch fracture toughness testing. *Engineering Fracture Mechanics* **2000**, 67(3), pp.263-76.

24. ASTM-E-399 Standard Test Method for Plane-Strain Fracture Toughness of Metallic Materials, E 399-90, 2003
25. Kuruppu, M.D. and Chong, K.P. Fracture toughness testing of brittle materials using semi-circular bend (SCB) specimen. *Engineering Fracture Mechanics* **2012**, *91*, pp.133-150.
26. Nakano, M. and Kishida, K. Measurement of dynamic fracture toughness by longitudinal impact of precracked round bar. *International Journal of Pressure Vessels and Piping* **1990**, *44*(1), pp.3-15.
27. Zhu, X.K. and Joyce, J.A. Review of fracture toughness (G, K, J, CTOD, CTOA) testing and standardization. *Engineering Fracture Mechanics* **2012**, *85*, pp.1-46.
28. Li, S., He, J., Gu, B., Zeng, D., Xia, Z.C., Zhao, Y. and Lin, Z. Anisotropic fracture of advanced high strength steel sheets: Experiment and theory. *International Journal of Plasticity* **2018**, *103*, pp.95-118.
29. Zrilic, M., Grabulov, V., Burzic, Z., Arsic, M. and Sedmak, S.. Static and impact crack properties of a high-strength steel welded joint. *International journal of pressure vessels and piping* **2007**,*84*(3), pp.139-150.